1984MNRAS.211..575H

Mon. Not. R. astr. Soc. (1984) **211**, 575–591

Gravitational lensing by cosmic strings

Craig Hogan★ and Ramesh Narayan† *Theoretical Astrophysics 130–33, California Institute of Technology, Pasadena, California 91125, USA*

Accepted 1984 June 20. Received 1984 June 11

Summary. We discuss the possible role of a cosmological distribution of vacuum strings in the gravitational imaging of quasars. Lensing properties are described for open strings and for large and small closed loops. A simplified model shows that small loops typically produce a pair of magnified merging images. This effect introduces an observational 'amplification bias' which causes magnified quasars to appear frequently in a flux-limited sample even though they are intrinsically rare. Highly magnified merging images are sensitive to small changes in the lens, and it is shown that loop oscillations can lead to observable variations in image size, configuration, and total luminosity. Furthermore, the functional form of this variability can be derived on the basis of universal properties of Lagrangian mappings near singularities. For example, the magnification varies as $m \propto |t - t_\infty|^{-1/2}$ where t_∞ is the time when the quasar crosses a caustic. At t_∞ the intensity becomes formally infinite, the two images merge and then suddenly vanish as the quasar passes to the other side of the caustic. The probability of observing lensing events with various properties are estimated in two simple scenarios, and the possibility of searching for them is discussed.

1 Introduction

Cosmic strings are topologically stable, one-dimensional defects in the vacuum which can appear during appropriate phase transitions in the early Universe. Strings associated with unified Yang–Mills theories are currently being studied as sources of the density fluctuations needed to produce galaxies and clusters of galaxies (Zeldovich 1980; Vilenkin 1981a, b; Turok 1984). In this paper, we consider the gravitational lensing properties of strings and investigate whether this phenomenon could be used to detect strings. Gott (1984) has recently considered this problem, but has concentrated mostly on open (infinitely long), nearly straight strings. Vilenkin (1984) has considered the additional effect of a loop population on lensing probabilities. We incorporate these effects into our model, and also

★ Bantrell Fellow.
† On leave from: Raman Research Institute, Bangalore 560080, India.

© Royal Astronomical Society • Provided by the NASA Astrophysics Data System

1984MNRAS.211..575H

include unique effects associated with relatively small string loops. We show that there can be significant magnification of the images and that therefore the effective cross-section for lensing by small loops could be comparable to that from open strings and large loops.

An important new effect discussed in this paper is that in certain cases the image intensities and separations can vary over a time-scale as short as a month. Flux increases with a characteristic power-law signature, terminating with a sudden disappearance of images; or conversely, bright quasars suddenly appear and then fade. These events are representative of a class of singularities of Lagrangian mappings, and their signature is related to universal properties of these singularities. We make order of magnitude estimates of the probability of occurrence of these effects and discuss the feasibility of looking for them.

We are motivated not only by the possibility of finding observable consequences of exotic cosmological relics, but also by the more pressing need to find a suitable explanation for the presently known cases of lensing. The current observational situation is ambiguous, but seems to suggest that known forms of mass concentration, such as ordinary galaxies or ordinary clusters of galaxies, may not be responsible for most of the observed instances of lensing. Cosmic strings have a number of properties which make them desirable alternative candidates.

We consider only strings which are forbidden to have ends, both because they are the simplest type and because strings which can terminate on a monopole of some sort tend to be short-lived. Thus the relic strings in the Universe may either be infinite open strings or closed loops. For the purposes of this paper there are two parameters that characterize the string population in the Universe. The most important is the mass per unit length μ, which we write in terms of the dimensionless parameter, ϵ,

$$\epsilon = G\mu/c^2. \tag{1.1}$$

The gravitational lensing effects of strings depend greatly on the magnitude of ϵ, larger values being more favourable. Currently, the observed degree of isotropy of the microwave background (Kaiser & Stebbins 1984), and the limit on gravitational radiation from the timing noise in the millisecond pulsar, suggest that $\epsilon \lesssim 10^{-5}$ (Hogan & Rees 1984). Secondly, when two strings cross, there is a probability $P_{\rm ic}$ that they can intercommute or switch partners. An open string that crosses itself and intercommutes produces a closed loop. Strings have extremely large internal tension ($P=-\rho$) and therefore curved strings experience accelerations to relativistic speeds while closed loops undergo relativistic oscillations. As we point out in Section 4 this has some very interesting consequences for image variability.

At any epoch in the Universe, we expect of order $P_{\rm ic}^{-1}$ open strings of length $\sim \pi ct$ and radius of curvature $\sim ct$ (where t is cosmic time) to lie within a sphere of radius ct (see e.g. Zeldovich 1980). The density in the Universe contributed by open strings is thus given by

$$\Omega_\infty \sim 2\pi\epsilon/P_{\rm ic}. \tag{1.2}$$

Strings that entered at an earlier epoch would have intercommuted to loops with a probability proportional to $P_{\rm ic}$, so the number of loops is not sensitive to $P_{\rm ic}$. Loops decouple from the expansion, and are also unlikely to intercommute further with the network of infinite strings, if they are smaller than the current horizon. After breaking off they suffer violent convulsions with possibly further intercommutations. It is likely that they eventually find a stable, nearly periodic non-self-intersecting trajectory (Kibble & Turok 1982). They lose energy primarily from gravitational radiation, and loops smaller than ϵct_0 have a lifetime less than the age t_0 of the Universe.

© Royal Astronomical Society • Provided by the NASA Astrophysics Data System

1984MNRAS.211..575H

In the rest of the paper we will, for convenience, assume that the lensing string is at a distance $ct_0/2$ from the observer and reduce all lengths to angular dimensions at this fiducial distance. Thus the angular loop radius R_{dec} below which there is a significant depletion of loop population due to gravitational radiation is

$$R_{dec} \sim 2\epsilon. \tag{1.3}$$

The Ω of the Universe in loops of angular radius R_l is estimated by assuming that approximately half a loop of radius ct separates out of the network in each volume of radius ct in a time interval $d \ln t$, yielding (see e.g. Vilenkin 1981a)

$$\frac{d\Omega_l}{d \ln R_l} \sim 2\pi\epsilon, \qquad R_l > R_{dec}$$
$$\sim 2\pi\epsilon(R_l/R_{dec}), \qquad R_l < R_{dec}. \tag{1.4}$$

In deriving the above it has been assumed that $R_{dec} > t_{eq}/t_0$, where t_{eq} corresponds to the transition from a radiation-dominated to a matter-dominated Universe. This is likely to be the case for all 'interesting' values of ϵ.

2 Gravitational lensing by infinite strings and large loops

An infinite string bends light passing in a perpendicular plane by an angle (Vilenkin 1981b)

$$\alpha_\infty = 4\pi\epsilon. \tag{2.1}$$

The bending is independent of the impact parameter (Fig. 1a). For a typical quasar at a (Newtonian) distance of ct_0 (i.e., twice as far as the lensing string at $ct_0/2$), the angular separation of the two images formed on either side of the string is then (see Fig. 2)

$$R_0 = 4\pi\epsilon. \tag{2.2}$$

Provided the radius of curvature of the string is much greater than R_0, which is most certainly the case for open strings, there is no amplification of the images. A string which is tilted from the plane of the sky by an angle θ would split images by $R_0 \cos\theta$, that is, tilted strings produce less bending. This variation has the opposite sense to what one would naïvely

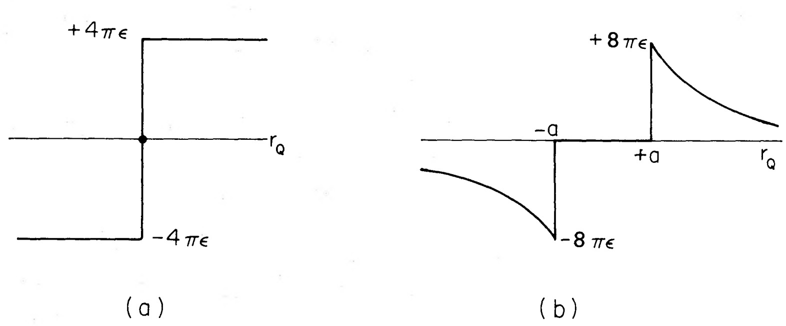

Figure 1. Bending angle for light passing by a stationary string in the plane of the sky, as a function of impact parameter. (a) shows bending by an infinite, straight, stationary string; rays on opposite sides are bent by $4\pi\epsilon$, independent of impact parameter, and there is a discontinuity at the string itself. (b) shows the effect of a static circular loop of reduced radius a. For impact parameter $r_Q > aR_0$, the loop has a Schwarzschild metric corresponding to the total loop mass (bending $\propto 1/r_Q$). There is again a discontinuity in bending at the string, and in this degenerate case there is no deflection in the interior of the loop.

© Royal Astronomical Society • Provided by the NASA Astrophysics Data System

1984MNRAS.211..575H

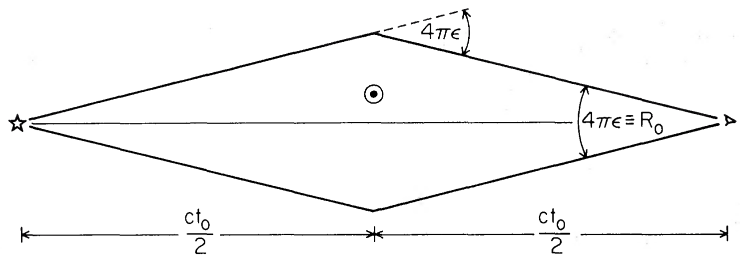

Figure 2. Bending by an open string at fiducial distance $ct_0/2$ with quasar at fiducial distance ct_0. Wit this geometry, the image separation is equal to the bending angle $4\pi\epsilon$, for rays perpendicular to th string. Ray paths do not change with transverse displacements of the string along a vertical line in thi figure, as long as the string remains between the rays.

expect for a Newtonian massive string (whose bending goes as $R_0 \sec\theta$). The difference i because of the peculiar 'conical' nature of spacetime around the string (Gott 1984).

Loops with a total angular length (at a distance $ct_0/2$) of $2\pi R_l$ would have formed a an epoch when their radius of curvature was $\sim R_l$ and it is not expected that wiggles o wavelength $\ll R_l$ would develop in their later evolution (Kibble & Turok 1982). It is there fore reasonable to suppose that the gravitational lensing properties of loops with $R_l > \beta R_0$ where β is some number between say 1 and 10, will be essentially similar to those of ope strings. In particular, no significant image amplification is expected from such loops.

To compute the cross-section for non-amplified lensing, we note from (1.4) that th angular length of open string expected within the horizon is $\sim 2\pi/P_{\rm ic}$ and that of loop with $R_l > \beta R_0$ is $\sim 2\pi \ln(2/\beta R_0) = 2\pi \ln(1/2\pi\epsilon\beta)$. The cross-section per unit length fo lensing is $\sim R_0$. Thus the probability of a given distant quasar at large redshift bein lensed is

$$P \sim (R_0/4\pi)[2\pi P_{\rm ic}^{-1} + 2\pi \ln(1/2\pi\epsilon\beta)] = 2\pi\epsilon[P_{\rm ic}^{-1} + \ln(1/2\pi\epsilon\beta)]. \quad (2.3$$

Except for small factors arising from differences in our simplified models, this estimat agrees with that of Vilenkin (1984).

3 Gravitational lensing by small loops

In this section we consider the lensing properties of idealized loops with circumferenc $2\pi R_l$ in the range $R_{\rm dec} \lesssim R_l \lesssim \beta R_0$. We study static loops in order to describe th dependence of various general features, such as the pattern of caustics, on the size an configuration of the lens. We assume that the gross features of these lensing events – especially the characteristic size of the pattern of caustics – carry over to the case of rapidly oscillating loop. Therefore in the next section we model the effect of the rapi motions of the loop by considering a sequence of these static configurations. This approxi mation is probably an adequate description of the *variation* so long as we confine ou attention to small continuous changes in the lens (i.e. the duration of the sequence is shor enough ($\ll R_l/c$) that the loop shape only changes by a small amount), and to types o lensing events whose local structure does not depend on any special properties of static o symmetric lenses.

Let us normalize all angles by $R_0 = 4\pi\epsilon$ and define the reduced loop radius

$$a = R_l/R_0, \qquad (1/2\pi) \lesssim a \lesssim \beta. \quad (3.1$$

To begin with, consider the case when the loop is perfectly circular and in the plane of th sky. The purpose of this exercise is not to model real lenses but to show that loops wit

© Royal Astronomical Society • Provided by the NASA Astrophysics Data System

1984MNRAS.211..575H

$a \sim 1$ routinely produce magnified images. A light ray travelling perpendicular to the plane of the loop at impact parameter R (reduced distance $r = R/R_0$) is deflected by an angle

$$\alpha(r) = 8\pi\epsilon a/r, \qquad r \gtrsim a \tag{3.2}$$

which corresponds to a reduced bending angle (α/R_0) of $2a/r$. (This behaviour at $r \gg a$ also holds for a real collapsing or expanding circular loop.) Rays passing through the loop are undeflected in this toy model (although in the realistic case there will be time-dependent deflection for rays with impact parameter $r \lesssim a$). Thus, the bending angle diagram looks as in Fig. 1b. Two cases can now be distinguished:

(1) $a > 1$. If the reduced projected radial position $r_Q (\equiv R_Q/R_0)$ of the quasar with respect to the centre of the loop lies in the range $(a-1) \leqslant r_Q \leqslant 1$, then two images are formed, one at the true position of the quasar and the other outside the loop at a radius

$$r_I = (r_Q/2) + [(r_Q/2)^2 + a]^{1/2}. \tag{3.3}$$

The first image is not magnified while the second is magnified by the factor

$$m = \left| \frac{r_I}{r_Q} \frac{dr_I}{dr_Q} \right|. \tag{3.4}$$

The maximum magnification occurs when $r_Q = a - 1$. Formally there is a third image located right on the loop, but this has zero magnification and is not seen. For $r_Q < (a-1)$ there is one image unaffected by the lens, while for $r_Q > a$, there is again only one image, with position and magnification as in (3.3) and (3.4).

(2) $a < 1$. For $r_Q > a$ there is one image and for $(1-a) \leqslant r_Q \leqslant 1$ there are two images, as in the previous case. However, for $r_Q < (1-a)$, three images will be formed, one on the quasar and the other two on either side of the loop. The position and magnification of one of the outer images, the one that occurs on the same side of the centre as the quasar, is given by (3.3) and (3.4). For the other image,

$$r_I = -(r_Q/2) + [(r_Q/2)^2 + a]^{1/2} \tag{3.5}$$

and the magnification is again (3.4). The magnifications of the two outer images diverge as $1/r_Q$ as $r_Q \to 0$. Despite the reduced cross-section which goes as r_Q^2, the increased magnification makes these events competitive with 'average' lensing events, as first pointed out by Turner, Ostriker & Gott (1984). However, we do not consider this in any further detail because of the very specialized assumptions we have made on the loop geometry.

The above discussion considers perfectly circular loops parallel to the plane of the sky. However, these are unlikely to occur in practice; in general we expect loops to be significantly distorted. A general treatment of the lensing by all possible configurations is clearly impossible. Nor is it likely to be very useful. However, it is reasonable to suppose that the generic behaviour of distorted loops can be investigated by studying the action of a monopole-like deflection (as in 3.2 for circular loops), *supplemented by a quadrupolar term.* The assumption here is that for rays passing outside the loop, a simple moment expansion of the bending, retaining only a few of the leading terms, has all the qualitative physics of the general situation. We will see below that for $a \lesssim 1$ imaging is not dominated by rays passing through the loop. Since the higher multipoles are weak, (both because the loop does not have any significant distortions with wavelengths $\ll R_l$ and because these terms fall off rapidly with distance) the model can be used for semi-quantitative estimates of the properties of generic lenses.

© Royal Astronomical Society • Provided by the NASA Astrophysics Data System

1984MNRAS.211..575H

Time variation due to the loop's oscillation is modelled by a time-varying quadrupole term, keeping the monopole component fixed. This is likely to be an adequate approximation to generic behaviour for observation times much shorter than a loop oscillation time. We do not attempt to solve here the general problem of light rays passing through the neighbourhood of a rapidly-oscillating loop. However, our main results do not rely on detailed knowledge of the string configuration since time variation is treated only in the neighbourhood of caustics (which have a universal structure for geometrical reasons), so the validity of the model in the short-duration limit only depends on the loop deformations being continuous. The quadrupole model is used primarily to normalize the spatial and temporal scale of caustics produced by loops in order to obtain somewhat better estimates of time-scales and probabilities than one would expect from a purely order-of-magnitude analysis. We have attempted to connect the model with actual loops only in degenerate cases (Appendix A).

Consider a loop of circumference $2\pi a$ with a projected quadrupole distortion orientated along the x and y axes. Let a ray pass outside the loop at $\mathbf{r} \equiv (r, \theta)$. In the presence of a quadrupole, the general form of the reduced projected vector bending $\eta(\mathbf{r}) \equiv \{\eta_r(\mathbf{r}), \eta_\theta(\mathbf{r})\}$ is given by

$$\eta_r(\mathbf{r}) = -\frac{a}{r} + \frac{2\gamma a^3}{r^3}\cos 2\theta \tag{3.6}$$

$$\eta_\theta(\mathbf{r}) = \frac{2\gamma a^3}{r^3}\sin 2\theta. \tag{3.7}$$

The $\cos 2\theta$ and $\sin 2\theta$ dependences describe the characteristic shearing action of a quadrupole and the r dependence is two powers steeper in the quadrupole term than in the monopole term a/r. The parameter γ measures the strength of the quadrupole relative to the monopole. Appendix A discusses some simple models and shows that γ is expected to be ~ 0.2 on the average. In estimating time variability we will assume that γ varies by about this amount in a light-crossing time for the loop.

The vector equation that solves for the positions $\mathbf{r}_\mathrm{I}$ of the images is

$$\mathbf{r}_\mathrm{Q} = \mathbf{r}_\mathrm{I} + \eta(\mathbf{r}_\mathrm{I}). \tag{3.8}$$

Nityananda & Ostriker (1984) have considered a similar problem (a point lens with a superposed weak r-independent shear) and computed the solutions for small γ. A key feature of their work is that there is a region near the centre of the lens, $r_\mathrm{Q} \lesssim \gamma$, within which a quasar is lensed into 5 images. As the quasar approaches the boundary of this region, two of the images approach each other, brightening as the inverse of their separation. The increased magnification enables one to see intrinsically fainter (and more numerous) quasars, and in a flux-limited sample of objects this effect tends to compensate for the reduced geometrical cross-section. These events can therefore be more important than one might have guessed from their cross-section only. Turner *et al.* (1984) first discussed this phenomenon, which they termed 'amplification bias'; a further discussion can be found in Narayan, Blandford & Nityananda (1984). We consider the question of amplification bias in greater detail in Section 5 in the context of the specific problem of loops.

Writing equation (3.8) in Cartesian coordinates

$$x_\mathrm{Q} = x_\mathrm{I} - \frac{a x_\mathrm{I}}{r_\mathrm{I}^2} - \frac{6\gamma a^3 x_\mathrm{I}}{r_\mathrm{I}^4} + \frac{8\gamma a^3 x_\mathrm{I}^3}{r_\mathrm{I}^6}, \tag{3.9}$$

$$y_\mathrm{Q} = y_\mathrm{I} - \frac{a y_\mathrm{I}}{r_\mathrm{I}^2} + \frac{6\gamma a^3 y_\mathrm{I}}{r_\mathrm{I}^4} - \frac{8\gamma a^3 y_\mathrm{I}^3}{r_\mathrm{I}^6}. \tag{3.10}$$

© Royal Astronomical Society • Provided by the NASA Astrophysics Data System

1984MNRAS.211..575H

The magnification $m(\mathbf{r}_\mathrm{I})$ of an image is given by the determinant of the Jacobian relating $\mathbf{r}_\mathrm{I}$ to $\mathbf{r}_\mathrm{Q}$. Thus

$$m(\mathbf{r}_\mathrm{I}) = J^{-1} = \left[\frac{\partial x_\mathrm{Q}}{\partial x_\mathrm{I}}\frac{\partial y_\mathrm{Q}}{\partial y_\mathrm{I}} - \frac{\partial x_\mathrm{Q}}{\partial y_\mathrm{I}}\frac{\partial y_\mathrm{Q}}{\partial x_\mathrm{I}}\right]^{-1} \tag{3.11a}$$

$$= \left[1 - \frac{a^2}{r_\mathrm{I}^4} + \frac{12\gamma a^4}{r_\mathrm{I}^6}\cos 2\theta_\mathrm{I} - \frac{36\gamma^2 a^6}{r_\mathrm{I}^8}\right]^{-1}. \tag{3.11b}$$

J goes to 0 on a closed curve in the r_I plane and this is the locus of merging infinite amplification images. Since J changes sign across this line, representing a flipping of the image parity, the two merging images of opposite parity approach each other from either side of the $J = 0$ line. There is similarly a closed curve in the $\mathbf{r}_\mathrm{Q}$ plane which gives the locus of quasar positions corresponding to infinite magnification. By reciprocity, this curve corresponds to the bright line/caustic which would appear on a screen at the quasar plane due to a light source at the observer. Fig. 3 shows typical examples of the $m \to \infty$ curves in the quasar and image planes.

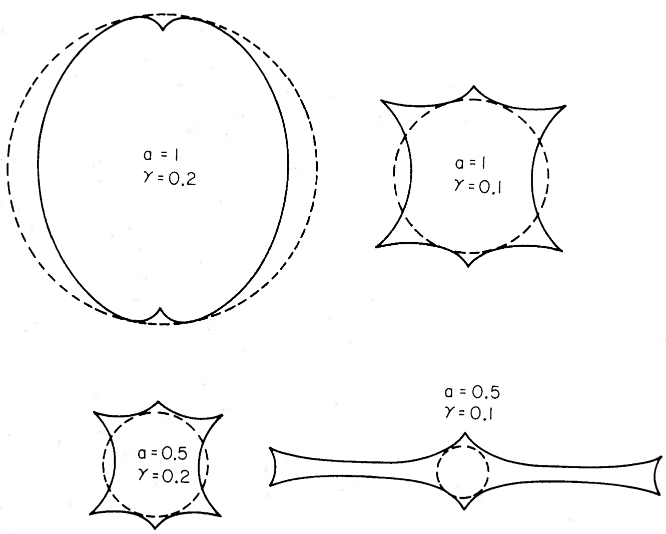

Figure 3a. Caustics (loci of quasar positions giving infinite magnification) in the quasar plane produced by the quadrupole lens model, for various values of the parameters a and γ. Dashed lines give the size (radius = $2\gamma a^{3/2}$) of equivalent circles adopted in estimating cross-sections for lensing.

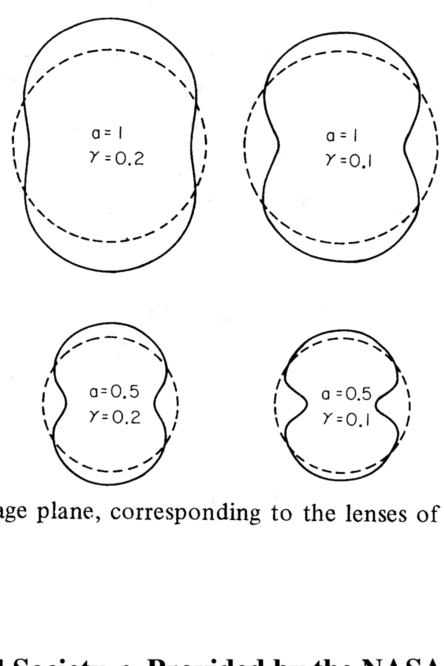

Figure 3b. Caustics in the image plane, corresponding to the lenses of Fig. 3a, with change of scale. The dashed circles have radius $a^{1/2}$.

© Royal Astronomical Society • Provided by the NASA Astrophysics Data System

1984MNRAS.211..575H

For analytic estimates, let us now assume γ to be small and neglect the γ^2 term in (3.11). Consider $\theta_I = \pi/4$, as a specific representative case. From (3.11), the merging images occur at the radial distance

$$r_{I,\infty} \sim a^{1/2}. \tag{3.12}$$

In general therefore, for $a \lesssim 1$ a significant fraction of the caustic appears outside the loop radius a, where we expect our quadrupole model to be representative of a large class of loops (see Fig. 3b); rays passing through the interior do not dominate the imaging. Substituting in (3.9) and (3.10), the corresponding quasar position is

$$-x_{Q,\infty} \sim y_{Q,\infty} \sim \sqrt{2}\gamma a^{3/2}; \qquad r_{Q,\infty} \sim 2\gamma a^{3/2}. \tag{3.13}$$

For the purpose of estimating cross-sections we will assume that the infinite magnification curves in the two planes are circles with the above radii, as shown in Fig. 3. This approximation errs on the conservative side in the sense that it tends to underestimate cross-sections at small a and γ.

4 Image structure near caustics: universality

Large amplification lensing events occur when the observer is near a caustic in the focal plane of the lens, that is, when the quasar is close to the singular curve in the $\mathbf{r}_Q$ plane. In situations like this we expect a universal behaviour characteristic of singularities of Lagrangian mappings. Of course, singularities of various types can occur (for example, the higher order 'cusps' in Fig. 3) but we will be concerned exclusively with the lowest-order 'fold' catastrophes in Thom's terminology (see Berry 1976), or singularities of type A_2 in Arnold's terminology (Arnold, Shandarin & Zeldovich 1982, see also Arnold 1984), because these will exhibit the generic behaviour of 'nearly all' high-amplification events. Zeldovich (1970) discussed a similar application of universality in the density profile around pancakes arising in 3-D collisionless flows. To our knowledge, universality in gravitational lensing was first studied by Nityananda (private communication). Here we introduce the idea that this universal behaviour might actually be observed in the time variability of quasars.

The relevance to strings is that since they move at the speed of light their caustics move quite rapidly, and we predict a universal time variability for amplified quasar images as the caustic moves past the quasar. For sufficiently large amplifications the time-scale for this variation may be short enough to be observable, because a very small displacement of the caustic can lead to a large variation in magnification. One can derive the detailed behaviour on the basis of scaling, using the following argument due to Nityananda. Consider the mapping between the Q-plane and the I-plane discussed in Section 3, and consider its behaviour in the neighbourhood of a caustic. If we orientate our coordinate axes normal to the caustic, the mapping is shown in Fig. 4. Universality arises from the parabolic character of the mapping. Amplification of paired images near the caustic is given by

$$m = (\partial \Delta r_Q / \partial \Delta r_I)^{-1} \tag{4.1}$$

as in (3.11), so that the probability $P(>m)$ that the magnification exceeds m is given by the probability $P(<\Delta r_Q) \propto \Delta r_Q$ that the quasar lies within the required Δr_Q of the caustic. Thus

$$P(>m) \propto m^{-2}, \tag{4.2}$$

a result found in specific models studied by Chang & Refsdal (1979), Turner *et al.* (1984), and Nityananda & Ostriker (1984).

© Royal Astronomical Society • Provided by the NASA Astrophysics Data System

1984MNRAS.211..575H

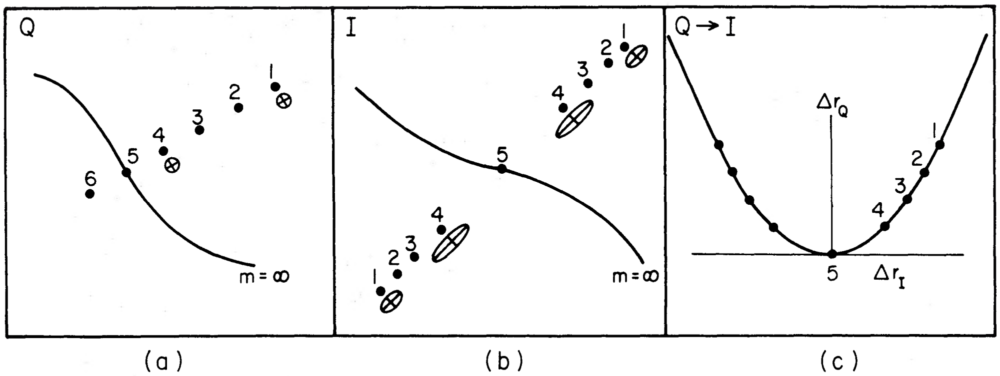

Figure 4. Imaging in the neighbourhood of a 'fold' catastrophe. The true projected position of the quasar is shown in the 'Q'-plane (a), while its apparent position appears in the 'I'-plane (b). The mapping between these planes (in a coordinate system orientated along the principal axis of the caustic in the Q-plane) is shown in (c). Universality arises from the parabolic character of the mapping near the caustic. Thus the image separation $2\Delta r_I$ varies as the square root of the displacement Δr_Q of the quasar from the caustic in the quasar plane. The points 1–6 correspond to various positions of the quasar; note that once the source has left the fold (point 6) there is no image at all. Magnification operates by mapping a given area element in the Q-plane to a larger area in the I-plane, stretching the two images along the line joining them, as shown in (b); lensing preserves surface brightness, but the increased solid angle of the image leads to a net magnification $m \propto \Delta r_I^{-1}$. Thus along this direction the angular size of the quasar is also magnified by m, enabling one to resolve much smaller scale structure in the quasar core than is normally possible.

Let us consider more quantitatively the nature of the solution in the neighbourhood of the infinite amplification events. For $r_Q > r_{Q,\infty}$, the merging images disappear altogether. This is characteristic of the 'fold catastrophe' which describes the present phenomenon (see Fig. 4). Therefore, let

$$r_Q = r_{Q,\infty}(1-\delta) \tag{4.3}$$

where we take $\delta \ll 1$. The merging images are then separated by a distance proportional to $\delta^{1/2}$. Scaling by $r_I \cong a^{1/2}$, the image separation $2\Delta r_I$ is thus

$$2\Delta r_I \sim (a\delta)^{1/2}. \tag{4.4}$$

The amplification of the images, which is proportional to $1/J$, varies as $1/\Delta r_I$. Now, for well separated images, i.e. $2\Delta r \sim r_I$, the amplification is $\sim r_I/r_Q$. Hence, the magnification of merging images is

$$m \sim 2\frac{r_I}{r_Q}\frac{r_I}{2\Delta r_I} \sim \frac{1}{\gamma a \delta^{1/2}} \tag{4.5}$$

where the factor of 2 takes into account the intensity of both (typically unresolved) images.

The movement of the string causes the caustics to move about. The centre of mass velocity of loops is much less than c, primarily because of the cosmological redshift of loop momentum since the time the loop was formed. However, internal loop oscillations are always very rapid and give rise to large amplitude shape variations on essentially a light-crossing time for the loop. Thus the imaging pattern changes on a time-scale $\propto a$. From (4.5) we see that as the caustic approaches the quasar, the image brightens as

$$m \propto |t - t_\infty|^{-1/2} \tag{4.6}$$

© Royal Astronomical Society • Provided by the NASA Astrophysics Data System

1984MNRAS.211..575H

until t_∞, when the brightness formally goes to infinity, the two images merge, and then suddenly disappear as the quasar crosses the caustic. The functional form of this variability is universal, and the time-scale $\tau \equiv |t - t_\infty|$ can be related to the amplification m as follows.

In our quadrupole model, τ at any instant is $\sim \Delta r_Q/r_Q$ times the light crossing time of the loop. Converting dimensionless angles back to lengths using the factor $R_0 ct_0/2 = 2\pi\epsilon ct_0$,

$$\tau \cong 2\pi a \epsilon t_0 \delta. \tag{4.7}$$

We substitute from (4.5) and express the result in terms of $m_3 \equiv m/1000$ (see Appendix B) and $\epsilon_{-6} \equiv \epsilon/10^{-6}$:

$$\tau \cong 1.6 m_3^{-2} a^{-1} \epsilon_{-6} h^{-1} \text{ yr} \tag{4.8}$$

where γ has been taken tobe 0.2 (Appendix A) and h is Hubble's constant in units of 100 km s^{-1} Mpc^{-1}. Similarly from (4.4) we have the image separation,

$$2\Delta r_I \cong 14 m_3^{-1} a^{-1/2} \epsilon_{-6} \text{ milliarcsec.} \tag{4.9}$$

The qualitative features of this behaviour in the neighbourhood of caustics are not influenced by our specific quadrupole model for the lens, although the numerical factors may differ somewhat for real loops. Interestingly, (4.8) and (4.9) can be combined to give the apparent transverse velocity v_I of the images at an assumed quasar distance ct_0,

$$v_I \cong \Delta r ct_0/\tau = 400 m_3 a^{1/2} c. \tag{4.10}$$

Thus, highly amplified merging images will in general have 'superluminal' motion, which by (4.9) can be easily resolved using VLBI if the quasar has a compact radio core. Furthermore, since the images are stretched by a factor of order m along the line joining them, the lens acts as a magnifying glass and enables one to resolve much smaller physical scales in the core, at least along this direction, within the merging images themselves.

Of course, the divergence at t_∞ only occurs for a perfect point source. In practice, quasars have a finite size (based on their intrinsic variability) of order 10^{-2} pc and the magnification saturates when Δr_Q is smaller than this:

$$m_{\max} \cong (\gamma a \delta_{\min}^{1/2})^{-1} \cong 4000 a^{-1/4} \epsilon_{-6}^{1/2} h^{1/2}, \tag{4.11}$$

This corresponds to a variability time-scale $\tau_{\min} \sim 0.1 a^{-1/2}$ yr which is naturally comparable to the intrinsic variability time-scale of the source. This is then also the time it takes for the 'sudden' appearance or disappearance to occur. At a magnification of ~ 4000 we expect even 10^{-3} pc structure in the core of a quasar to be resolved at milliarcsec resolution.

5 Amplification bias and probability of lensing by small loops

We are now in a position to estimate an effective cross-section for merger-type gravitational lensing by loops of a given a and γ. Consider the ring of r_Q corresponding to the range δ to $(\delta + d\delta)$ in (4.3). This has a physical angular area $\sim (2\gamma a^{3/2} R_0)^2\, 2\pi (d\delta)$. Quasars located in this ring are magnified by an amount given by (4.5). Because of the amplification, any magnitude-limited sample will preferentially detect such events (Turner *et al.* 1984). To quantify this effect, we need the luminosity function of quasars. Most current estimates suggest that a power-law behaviour holds, $\eta(>L_Q) \propto L_Q^{-\nu}$ with $\nu > 2$. Let us be conservative and use $\nu = 2$ (see Appendix B). Then, allowing for the amplification bias, the effective cross-section is m^2 times the geometrical cross-section, i.e.

$$d\sigma \sim \frac{8\pi\gamma^2 a^3 R_0^2 (d\delta)}{\gamma^2 a^2 \delta} = 8\pi R_0^2 a\, d(\ln \delta). \tag{5.1}$$

© Royal Astronomical Society • Provided by the NASA Astrophysics Data System

1984MNRAS.211..575H

Despite the fact that the physical area within which a quasar is lensed is $\sim r_Q^2 \sim \gamma^2 a^3$, the final effective cross-section is proportional to just a and so it is the total length of string in the loop that is important and not the details such as the actual radius or the strength of the quadrupole distortion. In this sense the result is very similar to that obtained in Section 3 where also we had a cross-section per unit string length. However, there is in addition an important new effect namely that equal logarithmic intervals of δ have equal cross-section. This is of course a consequence of the amplification bias. Let us take the range of $\ln \delta$ that contributes to the effective cross-section to be $\Lambda(\sim 10)$. Then the effective probability for the amplified events we have considered is

$$P \sim 8\pi\epsilon\Lambda \ln\ (2\pi\beta) \tag{5.2}$$

where the term $\ln(2\pi\beta)$ arises from integrating (1.4) over loop radii between $R_{\rm dec}$ and βR_0. Note the similarity of (5.2) to the cross-section $2\pi\epsilon \ln(1/2\pi\epsilon\beta)$ for large loops. The crucial difference is the extra factor of Λ which accounts for the amplification bias.

6 Models for string lensing

Combining the estimates (2.3) and (5.2), the total probability of a quasar being lensed by strings is approximately

$$P \cong 8\pi\epsilon\Lambda \ln(2\pi\beta) + 2\pi\epsilon \ln(1/2\pi\epsilon\beta) + 2\pi\epsilon P_{\rm ic}^{-1} \tag{6.1}$$

where the first term represents amplified events, the second contribution comes from the rest of the loop population (all loops from radius $2\pi\beta t_{\rm dec}$ up to t_0) and the third term comes from $P_{\rm ic}^{-1}$ open strings, each of which extends over $\simeq \pi$ radians in the sky.

We are now ready to construct specific scenarios for putting strings into the context of real lenses. There are currently five well established cases of gravitational lensing – Q0957+561 at quasar redshift $z_Q = 1.41$ with image separation $\Delta r_I = 6.2$ arcsec (Walsh, Carswell & Weymann 1979); Q1115+080, $z_Q = 1.72$, 4 images in a roughly circular pattern of diameter ~2.3 arcsec with two of the images roughly 3 mag brighter than the others and separated by only ~0.5 arcsec (Weymann *et al.* 1980); Q2035+007, $z_Q = 2.15$, $\Delta r_I = 7.3$ arcsec (Weymann, Green & Heckman 1982); Q2016+112, $z_Q = 3.27$, $\Delta r_I = 3.4$ arcsec (Lawrence *et al.* 1984); Q1635+267, $z_Q = 1.96$, $\Delta r_I = 3.8$ (Djorgovsky & Spinrad 1983). A giant galaxy and a cluster of galaxies have been seen at redshift 0.36 in the foreground of Q0957+561 and reasonable models have been proposed for the lensing geometry based on these (e.g., Young *et al.* 1981), but this is the only case which might be said to be well understood; several difficulties arise in the other cases.

A galaxy has been seen in the vicinity of Q2016+112 (Lawrence *et al.* 1984) and Q1115+080 (Henry, in preparation) but it is difficult to make reasonable models in these cases because of the peculiar location of the galaxies with respect to the images. Nothing resembling a galaxy lens has been seen in the other two cases, although deep CCD frames taken of these regions should have easily detected them (Narayan, Blandford & Nityananda 1984). The problem is aggravated by the fact that the fairly large $\Delta r_I > 2$ arcsec observed in all these cases seems to imply that fairly massive lenses are involved.

Apart from the above 5 cases, there are at least 3 other instances (Paczynski & Gorski 1981; Shaver & Robertson 1983; Surdej *et al.* 1983) of two or more quasars at essentially the same redshift (to within ~1000 km s^{-1}), separated by ~1 arcmin. These could be lensed images, though again no lens has been identified. In these cases the lens would need

© Royal Astronomical Society • Provided by the NASA Astrophysics Data System

1984MNRAS.211..575H

to be a system with a velocity dispersion of order $\sim 1500 \text{ km s}^{-1}$, corresponding to a fairly rich cluster of galaxies, which should be conspicuous on CCD frames out to redshifts of ~ 1.

In addition to all this there is the nagging problem that a lens with no singularities must always produce an odd number of images, whereas every known gravitational lens (including the 'triple' quasar) has an even number of images. In the absence of alternative explanations (such as obscuration of the odd image), this fact alone would lead one to suspect the existence of singular lenses (such as strings), in which the odd image can have zero intensity. Thus, in short, the observational situation is that several cases of gravitational lensing are known (or suspected), but there is no clear idea of what is causing the lensing, and no likely candidate appears to exist among known forms of mass concentration. It would therefore be interesting to see if cosmic strings have any role to play. We consider two possible scenarios below.

6.1 SCENARIO 1

Suppose the observed cases of lensing with image separation ~ 5 arcsec are unamplified lensing by single strings, i.e. pieces of open strings, or parts of large loops with $a \gg 1$. Then by (2.2)

$$\alpha_\infty = 4\pi\epsilon \simeq 5 \text{ arcsec} \quad \text{or} \quad \epsilon \simeq 2\times 10^{-6}. \tag{6.2}$$

Smaller image separations are possible if the strings are inclined at an angle to our line-of-sight, or if the lens is closer to the source instead of being located at the mid-point as in Fig. 2. Larger image separations of up to $8\pi\epsilon \cong 10$ arcsec are possible if the string is closer to the observer. For small loops with $a \lesssim 1$, the typical separation is $8\pi\epsilon$, and again could be smaller or larger than this depending on the orientation and location of the loop. Very much smaller separations are of course also possible in amplified events.

The lensing probability for non-amplified events is given by (6.1) with $\beta = 1$:

$$P \simeq 1.6\times 10^{-4} + 1.2\times 10^{-5} P_{\text{ic}}^{-1}. \tag{6.3}$$

One could hope to observe several such lensing events in a catalogue of a few thousand quasars only if P_{ic} is very small, say less than 10^{-2}. This seems a bit unlikely but is not impossible.

A prediction of this scenario is that we should observe amplified images with probability

$$P \cong 8\pi\epsilon\Lambda \ln(2\pi\beta) \simeq 10^{-4}\Lambda \tag{6.4}$$

where Λ may be ≈ 10 for all amplifications. However, Λ is only $\simeq 1$ for the probability that a quasar in a flux-limited sample varies by loop lensing between two monitorings separated by more than the τ corresponding to the amplification bias cut-off, which in this case corresponds to a few years (*cf.* 4.8). Thus, if we observe $\sim 10^4$ quasars for a few years, we should see one of them abruptly decrease in luminosity after a steady power-law increase with a time-scale of order a year.

The close pair of images in Q1115+080 would naturally be interpreted in this scenario as a merging pair, as seems to be indicated by their magnification relative to the other two images (Nityananda, private communication). According to (6.4), it is somewhat surprising that such an event should have been found; but this could be explained if our model of amplification bias were too conservative.

© Royal Astronomical Society • Provided by the NASA Astrophysics Data System

1984MNRAS.211..575H

6.2 SCENARIO 2

Here we suppose that the five certain cases of observed lensing are amplified merging images, caused by loops which have angular radius $\gg 5$ arcsec and at the same time have reduced radius $a \lesssim 1$ (this idea is similar to the suggestion by Narayan *et al.* 1984 that the known lensing events may be mergers caused by clusters of galaxies.) This scenario automatically requires a larger ϵ than the previous case. Let us take $4\pi\epsilon \simeq 1$ arcmin, i.e. $\epsilon \simeq 2.4 \times 10^{-5}$. Taking $a \sim 1$ the typical amplification for the observed images (from 4.9) is

$$m \sim 67\,(5\,\text{arcsec}/2\Delta r_{\mathrm{I}}). \tag{6.5}$$

The lensing probability is now

$$P \simeq 8\pi\epsilon\Lambda \ln(2\pi\beta) \simeq 10^{-3}\Lambda \tag{6.6}$$

which is about right to be compatible with the observed number of lenses.

The predictions here are:

(1) A substantial number of amplified lensing events should appear up to arcmin separations, with magnification inversely proportional to the image separation. The distribution of image separations is predicted to be nearly constant in each logarithmic interval of Δr_{I} for the assumed quasar luminosity function with $\nu = 2$ down to a minimum separation corresponding to the magnification where this luminosity function breaks down (see Appendix B).

(2) Unamplified lensing by infinite strings and loops with $a \gg 1$ will produce images of separation ~ 1 arcmin and would occur with probability $P \sim 10^{-3}$, so a number of quasars should have an image of approximately equal brightness $\simeq 1$ or 2 arcmin away (as noted also by Gott 1984 and Vilenkin 1984). Several candidates already exist for these 'wide-angle lenses,' as mentioned earlier.

(3) Events with observable variability time-scales should be about as frequent in optically selected samples as lensing events with arcsecond separation, if the amplification bias model used above is accurate at this large a magnification (*cf.* Appendix B). We predict that merging images with smaller Δr_{I}, if found (they may not be depending on the true luminosity function), should display universal time variability and the 'disappearing act' as described above, with probability now given by (6.6) rather than (6.4). Thus in this scenario, to observe variability one should observe only ~ 1000 quasars, but over a baseline of about 10 yr [from (4.8)] if we say that amplication bias works only up to $m \cong 1000$. The longer time-scale in this scenario is a direct consequence of the longer light crossing time for loops with $a \sim 1$. From (4.9), merging images should be easily observable using VLBI, with the image separation going as $\Delta r_{\mathrm{I}} \propto 1/m \propto \tau^{1/2}$. As noted in Section 4 such cases should provide a high-resolution picture of the quasar core along the axis joining the images.

Variation (including disappearing) is also happening on a much shorter time-scale down to $\tau_{\mathrm{min}} \sim 0.1$ yr, but for large m the probability is difficult to estimate because of uncertainty in the quasar luminosity function. If we compare the predictions of this model with scenario 1, we find that the larger ϵ makes large τ events more probable, whereas events with $\tau \sim 1$ yr may be roughly equally probable because the small-ϵ case requires less magnification to reach this short a time-scale so one may still take advantage of amplification bias.

Configurations such as Q1115+080 are more difficult to understand in this picture, and may require additional complications such as other lenses along the line-of-sight.

© Royal Astronomical Society • Provided by the NASA Astrophysics Data System

1984MNRAS.211..575H

7 Discussion

It is worthwhile to point out the connection between the effects discussed here and various other phenomena associated with cosmic strings.

(1) Loops predict a gravitational wave background $\Omega_g \simeq 2\pi\epsilon^{1/2}\Omega_{rad} \simeq 2\times 10^{-7}\epsilon_{-6}^{1/2}$. A value of $\epsilon \sim 10^{-5}$ is not quite ruled out but may eventually be so on the basis of timing measurements of the millisecond pulsar 1937+21 (Hogan & Rees 1984).

(2) Orbits around these loops can be quite fast; the velocity of a particle on a circular orbit around a loop is

$$\sqrt{2GM/R_l} \simeq 1000\epsilon_{-6}^{1/2}\ \mathrm{km\ s^{-1}}.$$

Stationary loops should have conspicuous effects on the matter distribution; one might expect hard X-rays if there is enough gas in the vicinity.

(3) An effect more directly related to lensing is that string motion leads to a characteristic discontinuity in the microwave background temperature of order (Kaiser & Stebbins 1984)

$$\delta T/T \simeq 4\pi\epsilon.$$

This can be searched for if a string is suspected of causing a particular lensing event. The predicted arcminute events of scenario 2 would be associated with strings whose discontinuities should be detectable with current equipment (Uson & Wilkinson 1984).

(4) Finally, there is the constraint that strings should produce sufficient density perturbations to lead to galaxy clustering. This predicts an ϵ which depends on the composition of the dark matter but cannot be less than $\sim 10^{-6}$.

One of the attractive features of strings as lenses (aside from the fact that they seem tc resolve a number of outstanding difficulties) is that once their existence is postulated, thei properties are theoretically well determined in an order of magnitude sense. The paramete ϵ determines the Ω in loops, their size distribution, variability time-scale, and characteristi bending angle. Independent constraints on ϵ such as those just mentioned may either rul out strings as candidate lenses or suggest that they should be taken seriously and their specia predictions searched for. Most of the important theoretical uncertainties (such as the exac probability of loop formation) are soluble in principle, and in any case do not enter strongl into all of the predicted effects.

A search for some of the spectacular time variation discussed in this paper is furthe motivated by the fact that many of the effects described here are also expected fo 'ordinary' (i.e. non-string) lenses. This is because the universal behaviour of the typ described here should appear in some context no matter what the lenses are; but estimate of probabilities depend on many factors which are very uncertain for objects whose proper ties are not as highly constrained theoretically as string loops. Rough estimates indicate tha time variability in ordinary lensing could indeed be observed down to time-scales of orde (size of quasar)/(velocity of lens relative to Earth–quasar line), which could be as short a tens of years.

It should be emphasized that the effect we are considering is quite distinct from variabilit caused by 'mini-lenses' (Chang & Refsdal 1979; Gott 1981). In the case of mini-lenses the natural time-scale of the phenomenon is itself short. In our scenario, the natural time scale for image variability is actually very long (in the case of loops it is $\sim 4\pi\epsilon t_0$), but i accelerated by the proximity of a caustic, and occurs even for a smooth lens. Since ordinar lenses have much smaller characteristic velocities than loops, they require a correspondingl larger magnification to obtain observably short time-scales. Therefore these events could b

© Royal Astronomical Society • Provided by the NASA Astrophysics Data System

1984MNRAS.211..575H

extremely rare if the amplification bias cuts off at some moderate magnification. However, since ordinary lenses have a much larger Ω than loops their overall lensing probability may still be substantial. Another issue to consider is whether mini-lenses, which occur in ordinary lenses but not in isolated strings, are likely to disrupt the smooth structure of the caustics. We intend to address some of these issues in future work.

It is clear that amplification bias, which is important for ordinary lenses, is also decisive in producing some of the most distinctive signatures of string lenses, especially the distribution of angular separations of images and the probability distribution of time variability. The greatest uncertainty in evaluating the observability of these effects, and in planning a realistic observing programme, lies in the present uncertainty regarding the quasar luminosity function at the very faint end. More precisely, what is needed is a better idea of the luminosity function of very compact sources (down to $\lesssim 10^{-2}$ pc) which are too faint to be classified as quasars.

According to present knowledge, it is not unreasonable to expect (particularly in scenario 2) an optically selected sample of a few thousand objects to reveal universal variability in several objects if a monitoring programme is carried out over ≈ 10 yr. (The monitoring may also be carried out in the radio at a frequency where most of the source luminosity typically comes from a region which subtends $\lesssim 1$ milliarcsec, but we have not investigated whether amplification bias works equally well for radio-selected samples.) Because of the characteristic power-law behaviour the shortest time-scale detected in any monitoring programme would typically correspond to the period elapsed between observations. It is probable most efficient to observe known sources and wait for them to amplify and disappear, although one can imagine supernova-search programmes being extended to search for the sudden appearance of quasar-like objects in the field with a power-law light curve.

Acknowledgments

It is a pleasure to thank Rajaram Nityananda for numerous discussions on the intricacies of gravitational lensing and for sharing with us his extensive unpublished work. Discussions with Richard Gott and Alexander Vilenkin are also gratefully acknowledged. This work was supported by the Bantrell Fellowship awarded to CH and by the National Science Foundation under grants AST 82-13001 and AST 82-14126.

References

Arnold, V. I., 1984. *Catastrophe Theory*, Springer-Verlag, Berlin.
Arnold, V. I., Shandarin, S. F. & Zeldovich, Ya. B., 1982. *Geophys. Astrophys. Fluid Dyn.*, **20**, 111.
Berry, M. V., 1976. *Adv. Phys.*, **25**, 1.
Chang, K. & Refsdal, S., 1979. *Nature*, **282**, 561.
Djorgovsky, S. & Spinrad, H., 1983. *Bull. Am. Astr. Soc.*, **15**, 937.
Fall, S. M., 1981. *The Structure and Evolution of Normal Galaxies*, p. 1, eds Fall, S. M. & Lynden-Bell, D., Cambridge University Press.
Gott, J. R., 1981. *Astrophys. J.*, **243**, 140.
Gott, J. R., 1984. Preprint, Princeton University.
Hogan, C. & Rees, M. J., 1984. *Nature*, in press.
Kaiser & Stebbins, 1984. *Nature*, **310**, *391*.
Kibble, T. W. B. & Turok, N., 1982. *Phys. Lett.*, **116B**, 141.
Lawrence, C. R., Schneider, D. P., Schmidt, M., Bennett, C. L., Hewitt, J. N., Burke, B. F., Turner, E. I. & Gunn, J. E., 1984. *Science*, **223**, 46.
Narayan, R., Blandford, R. & Nityananda, R., 1984. *Nature*, **310**, 112.
Nityananda, R. & Ostriker, J. P., 1984. *J. Astrophys. Astr.*, **5**, 235.
Paczynski, B. & Gorski, K., 1981. *Astrophys. J.*, **248**, L101.

© Royal Astronomical Society • Provided by the NASA Astrophysics Data System

1984MNRAS.211..575H

Schmidt, M. & Green, R. F., 1983. *Astrophys. J.*, **269**, 352.
Shaver, P. A. & Robertson, J. G., 1983. *Astrophys. J.*, **268**, L57.
Surdej, J., Swings, J. P., Henry, A., Arp, H., Kruszewski, A. & Pederson, H., 1983. *Quasars anc Gravitational Lenses, Proc. 24th Liege International Astrophysical Colloq.*, p. 355, ed. Swings, J. P. Université de Liège, Belgium.
Turner, E. L., Ostriker, J. P. & Gott, J. R., 1984. *Astrophys. J.*, in press.
Turok, N., 1984. Preprint, Institute for Theoretical Physics, Santa Barbara.
Uson, J. M. & Wilkinson, D. T., 1984. *Astrophys. J.*, **277**, L1.
Vilenkin, A., 1981a. *Phys. Rev. Lett.*, **46**, 1169.
Vilenkin, A., 1981b. *Phys. Rev. D.*, **24**, 2082.
Vilenkin, A., 1984. *Astrophys. J.*, **282**, L51.
Walsh, D., Carswell, R. F. & Weymann, R. J., 1979. *Nature*, **279**, 381.
Weymann, R. J., Green, R. F. & Heckman, T. M., 1982. *Astrophys. J.*, **255**, L5.
Weymann, R. J., Latham, D., Angel, J. R. P., Green, R. F., Liebert, J. W., Turnshek, D. A. & Tyson, J. A. 1980. *Nature*, **285**, 641.
Young, P., Gunn, J. E., Kristian, J., Oke, J. B. & Westphal, J. A., 1981. *Astrophys. J.*, **244**, 736.
Zeldovich, Ya. B., 1970. *Astr. Astrophys.*, **5**, 84.
Zeldovich, Ya. B., 1980. *Mon. Not. R. astr. Soc.*, **192**, 663.

Appendix A

We estimate the quadrupole parameter γ by considering two simple distortions of a loo of circumference $2\pi a$. For simplicity we will make a Newtonian analysis and take eac element dl of the loop to behave like a point mass μdl.

(1) Let us suppose the loop is fully stretched out into a straight string of length πa Consider the deflection at a distance r from the centre of the string along its axis. Up t quadrupolar order the bending is

$$\eta(r) = -\frac{1}{\pi}\int_{-\pi a/2}^{\pi a/2}\frac{dx}{(r-x)} \simeq -\frac{a}{r}-\frac{\pi^2 a^3}{24 r^3}. \qquad \text{(A.1}$$

Comparing with (3.6) this gives $|\gamma| = 0.41$ for this case.

(2) Let the loop be circular in shape with radius a but rotated out of the plane of th sky by an angle θ. Once again consider a point at a distance r from the centre of the loo along the long axis of the projected ellipse.

$$\eta(r) = \frac{1}{2\pi}\int_0^{2\pi}\frac{a\,d\phi(r-a\cos\phi)}{[(r-a\cos\phi)^2+a^2\sin^2\phi\cos^2\theta]} \simeq -\frac{a}{r}-\frac{a^3\sin^2\theta}{2r^3}. \qquad \text{(A.}$$

Thus $\gamma = 0.25\sin^2\theta$.

Using these values as a guide we take $\gamma = 0.2$ in all the numerical estimates in this paper.

Appendix B

The following discussion of the quasar luminosity function is based on the work of Schmi & Green (1983). Leaving out Q 2016+116 which is radio selected, the mean appare magnitude of the brightest image in the other 4 known cases of gravitational lensing $m \sim 18$, which corresponds to an absolute magnitude at $z_Q = 2$ of $M_B \simeq -26.5$ (f $h = 1$), assuming no amplification. At this redshift and intrinsic luminosity, Schmidt Green estimate the number density of quasars to be

$$\frac{d\Phi}{dM} \sim 80\ \text{Gpc}^{-3}. \qquad \text{(B}$$

© Royal Astronomical Society • Provided by the NASA Astrophysics Data System

1984MNRAS.211..575H

The slope of the luminosity function at $M_B = -26.5$ is ~ -2.8 at $z_Q = 1.5$ and ~ -2.5 at $z_Q = 2.5$; however, the curve flattens out at fainter magnitudes. We therefore conservatively take an average slope of -2 over the whole range of L

$$\text{i.e.} \quad \Phi(>L) \propto L^{-2}. \tag{B2}$$

A crucial question is: how far down does this luminosity function extend? Let us arbitrarily cut it off at that $L_{\rm min}$ at which $\Phi(>L_{\rm min})$ becomes equal to the number density of normal L^* galaxies (which is 1.9×10^7 Gpc^{-3} according to Fall 1981). This corresponds to a faintest quasar magnitude of $M_B = -19.5$ and a maximum magnification of 7 mag, i.e, a factor of ~ 650. For a pair of unresolved merging images, the maximum magnification is thus $\gtrsim 1000$.

© Royal Astronomical Society • Provided by the NASA Astrophysics Data System